

Selective Catalytic Oxidation of Ammonia to Nitrogen over Fe₂O₃–TiO₂ Prepared with a Sol–Gel Method

R. Q. Long and R. T. Yang¹

Department of Chemical Engineering, University of Michigan, Ann Arbor, Michigan 48109-2136

Received May 17, 2001; revised January 30, 2002; accepted January 30, 2002

Fe₂O₃–Al₂O₃, Fe₂O₃–TiO₂, Fe₂O₃–ZrO₂, and Fe₂O₃–SiO₂ were prepared with a sol–gel method and they showed high activities for selective catalytic oxidation (SCO) of ammonia to nitrogen in the presence of excess oxygen. The Fe₂O₃–TiO₂ catalysts prepared from iron sulfate yielded a higher selectivity for N₂ than those prepared from nitrate. More than 92% of N₂ yields were obtained on the 10 wt% Fe₂O₃–TiO₂ (SO₄²⁻) and 20 wt% Fe₂O₃–TiO₂ (SO₄²⁻) at 400–450°C under the condition of GHSV = 2.0 × 10⁵ h⁻¹. Also, after the Fe₂O₃–TiO₂ prepared from nitrate was treated with SO₂ + O₂ at 450°C, the N₂ selectivity and yield were enhanced significantly at 450–500°C, suggesting a promoting role by SO₂. But H₂O decreased the N₂ yield slightly. The N₂ selectivity for the SCO reaction is in good agreement with their surface acidity and the activity for selective catalytic reduction (SCR) of NO with ammonia. This further supports the two-step SCO mechanism in which NH₃ is first oxidized to NO and then NO is reduced to N₂ by unreacted NH₃ adsorbed species through a SCR reaction. The presence of sulfate species on Fe₂O₃–TiO₂ (SO₄²⁻) increased surface acidity and thus improved SCO performance. Temperature-programmed desorption and temperature-programmed surface reaction of ammonia showed that gaseous, adsorbed, and lattice oxygen may participate in the SCO reaction. © 2002 Elsevier Science (USA)

Key Words: selective catalytic oxidation (SCO) of NH₃; selective catalytic reduction (SCR) of NO; Fe₂O₃–TiO₂; sol–gel.

INTRODUCTION

The removal of ammonia from waste streams is becoming an increasingly important problem. It is known that many chemical processes use reactants containing ammonia or produce ammonia as a by-product. They are all plagued with ammonia slip problem. Selective catalytic oxidation (SCO) of ammonia to nitrogen is potentially an ideal technology for removing ammonia from oxygen-containing waste gases and consequently it has become of increasing interest in recent years (1–11). Moreover, ammonia is used effectively in power plants for NO_x (x = 1, 2) abatement by selective catalytic reduction (SCR, 4NH₃ + 4NO + O₂ =

4N₂ + 6H₂O). The commercial catalysts that are used today are V₂O₅ + WO₃ (or MoO₃) supported on TiO₂ (12). In order to control ammonia slip, most processes are carried out under the conditions such that NH₃/NO < 1 (≈0.9), which results in a decrease in NO reduction efficiency. For improving the NO reduction efficiency, the use of a stoichiometric or excess amount of ammonia is desirable. The SCO of ammonia can be applied to the SCR of NO in a secondary bed to oxidize the residual ammonia to N₂, without introducing other reactants into the gas mixture. The SCO process can also be applied to the combustion of biomass-derived gases for removing the NH₃ impurity (3, 4).

Several types of materials have been reported to be active for SCO of ammonia to N₂, such as Pt, Rh, and Pd exchanged to ZSM-5 (2); Ni, Fe, and Mn oxides supported on γ-Al₂O₃ (3, 4), V₂O₅/TiO₂, CuO/TiO₂, and Cu–ZSM-5 (5); CuO/Al₂O₃ (6, 7); Cu–Mn/TiO₂ (8); Fe-exchanged TiO₂-pillared clay (9); and Fe-exchanged ZSM-5 and other zeolites (10, 11). These catalysts exhibited activities for N₂ formation under various conditions. Amblard *et al.* (3) reported that among transition metal oxides supported on γ-Al₂O₃, Ni/Al₂O₃, Mn/Al₂O₃, and Fe/Al₂O₃ were the most active and selective catalysts for the SCO reaction. In our previous work (10), we studied the SCO reaction on a series of transition-metal (Cr, Mn, Fe, Co, Ni, Cu, and Pd) ion-exchanged zeolites. Results showed that the catalytic performance (i.e., NH₃ conversion and N₂ selectivity) increased in the trend of Co–ZSM-5 ≈ Ni–ZSM-5 < Mn–ZSM-5 < H–ZSM-5 < Pd–ZSM-5 < Cr–ZSM-5 < Cu–ZSM-5 < Fe–ZSM-5 at a high gas hourly space velocity (GHSV = 2.3 × 10⁵ h⁻¹). In particular, near 100% of NH₃ conversion to N₂ was obtained at 450°C on the Fe–ZSM-5. H₂O and/or SO₂ decreased the NH₃ conversion only slightly (10). Also, we found that there existed a good correlation between the N₂ selectivity for the SCO reaction and the activity for the SCR of NO with ammonia for the Fe-exchanged zeolites, i.e., the higher the SCR activity, the higher the N₂ selectivity in the SCO (11). This supported the SCO mechanism involving NO as an intermediate for N₂ formation.

¹To whom correspondence should be addressed. E-mail: yang@umich.edu.

In this work, we studied the SCO performance over Fe₂O₃-TiO₂ mixed oxides. The catalysts were prepared through a sol-gel route, using iron nitrate and iron sulfate as iron precursors. It is known that the sol-gel technique can result in a better iron dispersion than conventional impregnation methods. Also, the effect of water on the SCO performance and the correlation between SCO performance (N₂ selectivity) and SCR activity were studied. Temperature-programmed desorption (TPD) and temperature-programmed surface reaction (TPSR) were used to investigate ammonia adsorption and the reaction between ammonia adsorbed species and oxygen.

EXPERIMENTAL

Preparation of catalyst. The mixed oxides were prepared by a one-step sol-gel technique. In each case, a certain amount of iron nitrate or sulfate was first dissolved in 70 ml of methanol (1.7 mol) and then 0.05 mol of titanium butoxide (or zirconium butoxide, aluminum butoxide, and silicon ethoxide) was added into the solution with stirring. Subsequently, 3 ml of a 0.2 M HNO₃ solution was added dropwise into the mixture and stirred for hydrolysis and gelation. After the gelation was completed, the gel was aged for 2 days at room temperature and then calcined at 500°C for 6 h in flowing O₂ (150 ml/min). Finally, the samples were crushed and sieved to 60–100 mesh. The Fe₂O₃ amounts in the mixed oxides were controlled at 1–20% by weight. Since significant amounts of sulfate species still existed on the catalysts that were prepared from iron sulfate (see Fig. 1), the catalysts are expressed as Fe₂O₃-TiO₂ (SO₄²⁻). Fe(NO₃)₃·9H₂O (98%), Fe₂(SO₄)₃·7H₂O (98%), methanol (99.9%), and aluminum butoxide (97%) were supplied from Aldrich. Titanium butoxide (98+%), zirconium butoxide (78% in *n*-butanol), and silicon ethoxide (98%) were obtained from Strem Chemicals.

Characterization of catalyst. A Micromeritics ASAP 2010 micropore size analyzer was used to measure the N₂ adsorption isotherms of the samples at liquid N₂ temperature (-196°C). The specific surface area was determined from the linear portion of the BET plot ($P/P_0 = 0.05$ – 0.20). The pore size distribution was calculated from the desorption branch of the N₂ adsorption isotherm using the Barrett-Joyner-Halenda (BJH) formula. Prior to the surface area and pore size distribution measurements, the samples were degassed in vacuum at 350°C for 6 h.

The mixed oxides were also investigated by FTIR spectroscopy on a Nicolet Impact 400 FTIR spectrometer with a TGS detector. In each experiment, the catalyst was first mixed with KBr at a ratio of 1/9 (by weight). A self-supporting wafer with a 1.3-cm diameter was prepared by pressing 30 mg of the mixture and was then loaded into an IR cell with BaF₂ windows. The spectra were recorded at room temperature by accumulating 100 scans at a spec-

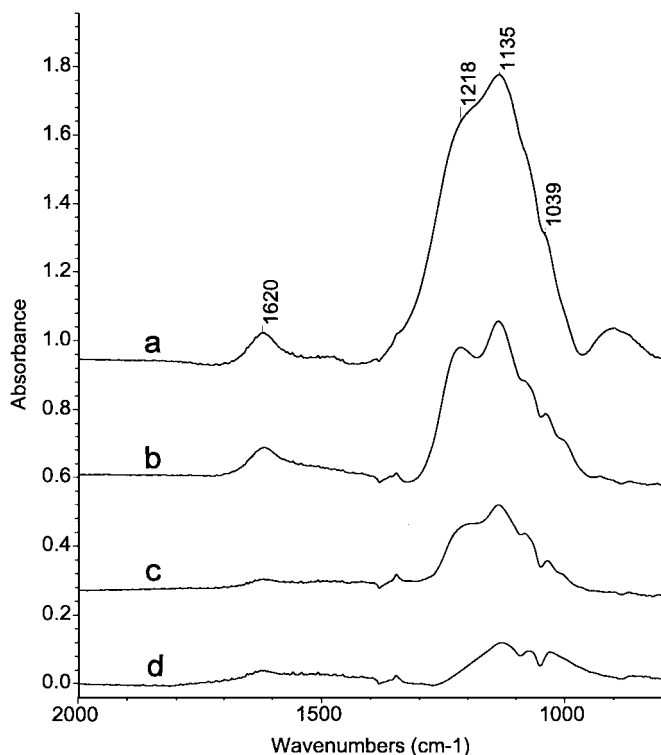


FIG. 1. FTIR spectra of sulfate species on (a) 20, (b) 10, (c) 5, and (d) 1% Fe₂O₃-TiO₂ (SO₄²⁻) catalysts at room temperature.

tral resolution of 4 cm⁻¹, using the empty cell as background.

SCO performance. The SCO activity measurement was carried out in a fixed-bed quartz reactor. The reaction temperature was controlled by an Omega (CN-2010) programmable temperature controller, and in this work 0.2 g catalyst was used. The reactant gas was obtained by blending different gas flows. The typical reactant gas composition was as follows: 1000 ppm NH₃, 2% O₂, 2.5% H₂O (when used), and balance He. The total flow rate was 500 ml/min (ambient conditions) and thus a high gas hourly space velocity (GHSV = 2.0×10^5 h⁻¹) was obtained. Premixed 1.07% NH₃ in He (with 0.05% H₂O as impurity) was supplied by Matheson. Water vapor was generated by passing He through a gas-wash bottle containing deionized water. A magnetic-deflection-type mass spectrometer (AERO VACTM, Vacuum Technology, Inc.) was used to monitor continuously the effluent gas from the reactor, which contained NH₃ ($m/e = 17$ minus the contribution of H₂O), H₂O ($m/e = 18$), N₂ ($m/e = 28$), NO ($m/e = 30$), O₂ ($m/e = 32$), and N₂O ($m/e = 44$). NO₂ ($m/e = 46$) was not detectable with this mass spectrometer. The concentrations of NH₃ and formed NO_x were also continually monitored with a chemiluminescent NO/NO_x analyzer (Model 42C, Thermo Environmental Instruments, Inc.), in which a high-temperature converter converted NH₃ to NO_x by the

reaction $\text{NH}_3 + \text{O}_2 \rightarrow \text{NO}_x + \text{H}_2\text{O}$. The NH_3 conversion was calculated by $([\text{NO}] + 2[\text{N}_2] + 2[\text{N}_2\text{O}])/[\text{NH}_3]_0 \times 100\%$, where $[\text{NH}_3]_0$ is the initial NH_3 concentration. The selectivity is defined as the percentage conversion of ammonia to N_2 , N_2O , and NO . The data were collected when the SCO reaction reached the steady state, typically after 20 min at each temperature.

SCR performance. The SCR activity measurement was carried out in the same fixed-bed quartz reactor. The reaction conditions were as follows: 0.2 g of catalyst, 1000 ppm NO , 1000 ppm NH_3 , 2% O_2 , and balance He . The total flow rate was 500 ml/min (ambient conditions). Premixed 1.01% NO/He was supplied by Matheson. The NO and NO_2 concentrations were continually monitored by the chemiluminescent NO/NO_x analyzer. To avoid errors caused by the oxidation of ammonia in the converter of the NO/NO_x analyzer, an ammonia trap containing phosphoric acid solution was installed before the sample inlet to the chemiluminescent analyzer. All the data were obtained after 20 min, when the SCR reaction reached steady state.

TPD and TPSR analyses. TPD and TPSR experiments were carried out in a fixed-bed quartz reactor. Before the experiment, 0.5 g of sample was pretreated in He at 500°C for 30 min to remove adsorbed H_2O and other gases. After the sample was cooled to room temperature, the He flow was switched to a flow of 1.07% NH_3/He for 60 min (100 ml/min). Mass spectra showed that the intensity of ammonia had stabilized. The sample was then purged by He (200 ml/min) for another 30 min. For the TPD experiment, He was passed through the reactor and ammonia TPD was performed by ramping the temperature at $10^\circ\text{C}/\text{min}$ to 500°C . For the TPSR experiments, subsequent to the ammonia adsorption step, the He flow was switched to 5% O_2/He (200 ml/min). At the same time, the reactor was heated linearly at $10^\circ\text{C}/\text{min}$ to 500°C . The magnetic-deflection-type mass spectrometer was used to monitor continuously the effluent gas from the reactor, which contained NH_3 , H_2O , N_2 , NO , O_2 , and N_2O .

RESULTS

Main characteristics of catalysts. The BET surface area, pore volume, and pore size of Fe_2O_3 -containing mixed oxides are summarized in Table 1. The mixed oxides prepared with the sol-gel method showed high surface areas, except $\text{Fe}_2\text{O}_3\text{-SiO}_2$. The surface area and pore volume decreased in a sequence of $\text{Fe}_2\text{O}_3\text{-Al}_2\text{O}_3 > \text{Fe}_2\text{O}_3\text{-TiO}_2$, $\text{Fe}_2\text{O}_3\text{-ZrO}_2 > \text{Fe}_2\text{O}_3\text{-SiO}_2$. The average pore diameters in these catalysts were 3.6–11.9 nm.

The IR spectra of the $\text{Fe}_2\text{O}_3\text{-TiO}_2$ prepared with iron sulfate are shown in Fig. 1. Four IR bands were observed at 1620, 1218, 1135, and 1039 cm^{-1} . The 1620-cm^{-1} band is assigned to adsorbed H_2O on the surface, whereas the other bands are attributed to the bidentate sulfate coordi-

TABLE 1
Characterization of the Catalysts

Sample	BET surface area (m^2/g)	Pore volume (cm^3/g)	Average pore diameter (nm)
5% $\text{Fe}_2\text{O}_3\text{-Al}_2\text{O}_3$	245	1.10	11.9
5% $\text{Fe}_2\text{O}_3\text{-TiO}_2$	104	0.14	3.7
5% $\text{Fe}_2\text{O}_3\text{-ZrO}_2$	106	0.14	3.8
5% $\text{Fe}_2\text{O}_3\text{-SiO}_2$	29	0.04	6.0
1% $\text{Fe}_2\text{O}_3\text{-TiO}_2(\text{SO}_4^{2-})$	97	0.18	4.6
5% $\text{Fe}_2\text{O}_3\text{-TiO}_2(\text{SO}_4^{2-})$	98	0.14	3.9
10% $\text{Fe}_2\text{O}_3\text{-TiO}_2(\text{SO}_4^{2-})$	106	0.19	3.6
20% $\text{Fe}_2\text{O}_3\text{-TiO}_2(\text{SO}_4^{2-})$	92	0.14	3.9

nated to Fe and/or Ti sites (13). This indicates that significant amounts of sulfate species still existed on the catalysts after calcination at 500°C . Since sulfated TiO_2 and sulfated Fe_2O_3 show similar IR bands at 1210–1230, 1130–1150, and $1030\text{--}1060\text{ cm}^{-1}$, it is difficult to determine to which sites the sulfate species were bonded by IR spectroscopy (13). However, our previous work indicated that Fe_2O_3 was sulfated more easily than TiO_2 (14). Also the sulfate amount decreased with decreasing Fe_2O_3 content. Hence it is reasonable to conclude that the sulfate species were bonded mainly to iron sites of $\text{Fe}_2\text{O}_3\text{-TiO}_2(\text{SO}_4^{2-})$. By comparison, no IR bands at $1500\text{--}1300\text{ cm}^{-1}$ due to nitrate species were observed on the Fe_2O_3 -containing mixed oxides that were prepared with iron nitrate. Iron nitrate was decomposed to iron oxide in the process of calcination.

SCO performance on Fe_2O_3 -containing catalysts. The SCO performance of Fe_2O_3 -containing catalysts prepared with iron nitrate is summarized in Table 2. Under the conditions of 1000 ppm NH_3 , 2% O_2 , and $\text{GHSV} = 2.0 \times 10^5\text{ h}^{-1}$, the mixed oxides showed various catalytic performance at different temperatures. NH_3 conversion increased with reaction temperature and all of the catalysts showed very high NH_3 conversions at high temperatures. In all cases, N_2 , NO , and H_2O were the products for ammonia oxidation. N_2O formation was not observed. At low temperatures, N_2 was the main product. With increasing temperature, N_2 selectivity decreased, whereas NO selectivity increased significantly. The maximum N_2 yield on the Fe_2O_3 -containing catalysts decreased in the order of $\text{Fe}_2\text{O}_3\text{-Al}_2\text{O}_3 > \text{Fe}_2\text{O}_3\text{-TiO}_2 > \text{Fe}_2\text{O}_3\text{-ZrO}_2 > \text{Fe}_2\text{O}_3\text{-SiO}_2$.

SCO performance on $\text{Fe}_2\text{O}_3\text{-TiO}_2(\text{SO}_4^{2-})$ catalysts. The SCO performance of 1–20% $\text{Fe}_2\text{O}_3\text{-TiO}_2$ prepared from iron sulfate is summarized in Table 3. These catalysts also showed near 100% NH_3 conversions at high temperatures. N_2 and NO were the oxidation products. By comparison, these catalysts showed much higher N_2 selectivity than those prepared from iron nitrate (Table 2). This was related to the fact that sulfate species are present on the catalyst, as shown by the above IR spectra (Fig. 1). This point has been verified by a separate experiment. When the 5%

TABLE 2
Catalytic Performance of 5% Fe₂O₃-Containing Catalysts for SCO of NH₃^a

Catalyst	Temperature (°C)	NH ₃ conversion (%)	Selectivity (%)		N ₂ yield (%)
			N ₂	NO	
Fe ₂ O ₃ -TiO ₂	300	39	91	9	35
	350	65	78	22	51
	400	89	74	26	66
	450	97	76	24	74
	500	99	62	38	61
Fe ₂ O ₃ -ZrO ₂	300	34	94	6	32
	350	62	80	20	50
	400	83	74	26	61
	450	92	77	23	71
	500	95	61	39	58
Fe ₂ O ₃ -Al ₂ O ₃	300	38	93	7	35
	350	68	80	20	54
	400	85	78	22	66
	450	96	81	19	78
	500	97	71	29	69
Fe ₂ O ₃ -SiO ₂	300	24	94	6	23
	350	47	79	21	37
	400	84	70	30	59
	450	95	65	35	62
	500	98	51	49	50

^a Reaction conditions: 0.2 g of catalyst, [NH₃] = 1000 ppm, [O₂] = 2%, He = balance, total flowrate = 500 ml/min, and GHSV = 2.0 × 10⁵ h⁻¹.

TABLE 3
Catalytic Performance of Fe₂O₃-TiO₂(SO₄²⁻) Catalysts for SCO of NH₃^a

Catalyst	Temperature (°C)	NH ₃ conversion (%)	Selectivity (%)		N ₂ yield (%)
			N ₂	NO	
1% Fe ₂ O ₃ -TiO ₂ (SO ₄ ²⁻)	300	37	91	9	34
	350	83	78	22	65
	400	98	80	20	78
	450	99	75	25	74
	500	99	52	48	51
5% Fe ₂ O ₃ -TiO ₂ (SO ₄ ²⁻)	300	19	95	5	18
	350	62	86	14	53
	400	98	91	9	89
	450	99	77	23	76
	500	99	59	41	58
10% Fe ₂ O ₃ -TiO ₂ (SO ₄ ²⁻)	300	17	94	6	16
	350	51	92	8	47
	400	97	96	4	93
	450	99	95	5	94
	500	99	72	28	71
20% Fe ₂ O ₃ -TiO ₂ (SO ₄ ²⁻)	300	18	94	6	17
	350	52	93	7	48
	400	98	94	6	92
	450	99	93	7	92
	500	99	72	28	71

^a Reaction conditions: 0.2 g of catalyst, [NH₃] = 1000 ppm, [O₂] = 2%, He = balance, total flow rate = 500 ml/min, and GHSV = 2.0 × 10⁵ h⁻¹.

Fe₂O₃-TiO₂ prepared from iron nitrate was treated with 500 ppm SO₂ + 10% O₂ (250 ml/min) at 450°C for 1 h, N₂ selectivity increased from 62–76% to 90–92% at 450–500°C (with a slight decrease in NH₃ conversion from 97–99% to 87–98%). This results in an increase in N₂ yield from 61–74% to 80–89%, suggesting a promoting role by sulfation for N₂ formation. For Fe₂O₃-TiO₂ (SO₄²⁻), with increasing Fe₂O₃ content (also sulfate content) from 1% to 10%, N₂ selectivity and yield increased significantly (Table 3). Further increase in iron and sulfur contents did not increase N₂ selectivity and yield at high temperatures. More than 92% of N₂ yields were obtained on the 10% Fe₂O₃-TiO₂ (SO₄²⁻) and 20% Fe₂O₃-TiO₂ (SO₄²⁻) at 400–450°C.

Effect of H₂O on SCO performance. It is known that the waste streams usually contain water vapor. We further studied the effects of H₂O on the SCO performance of Fe₂O₃-TiO₂ (SO₄²⁻) catalysts (Table 4). When 2.5% H₂O was added to the reactants, it can be seen by comparing Tables 3 and 4 that N₂ selectivities were almost unchanged at low temperatures, but decreased slightly at high temperatures. The NH₃ conversion was increased by water vapor at low temperatures. Overall, the N₂ yield decreased slightly in the presence of H₂O. Also, in the presence of water vapor, the maximum N₂ yield increased with increasing iron and sulfur contents over the 1–20% Fe₂O₃-TiO₂ (SO₄²⁻) catalysts.

TABLE 4
Effect of H₂O on Catalytic Performance of Fe₂O₃-TiO₂(SO₄²⁻) Catalysts for SCO of NH₃^a

Catalyst	Temperature (°C)	NH ₃ conversion (%)	Selectivity (%)		N ₂ yield (%)
			N ₂	NO	
1% Fe ₂ O ₃ -TiO ₂ (SO ₄ ²⁻)	300	44	91	9	40
	350	87	75	25	65
	400	97	74	26	72
	450	99	73	27	72
	500	99	51	49	50
5% Fe ₂ O ₃ -TiO ₂ (SO ₄ ²⁻)	300	32	94	6	30
	350	78	83	17	65
	400	93	85	15	79
	450	96	77	23	74
	500	99	59	41	58
10% Fe ₂ O ₃ -TiO ₂ (SO ₄ ²⁻)	300	36	95	5	34
	350	51	92	8	47
	400	97	86	14	83
	450	99	71	29	70
	500	99	65	35	64
20% Fe ₂ O ₃ -TiO ₂ (SO ₄ ²⁻)	300	21	97	3	20
	350	52	89	11	46
	400	94	87	13	82
	450	99	87	13	86
	500	99	71	29	70

^a Reaction conditions: 0.2 g of catalyst, [NH₃] = 1000 ppm, [O₂] = 2%, [H₂O] = 2.5%, He = balance, total flow rate = 500 ml/min, and GHSV = 2.0 × 10⁵ h⁻¹.

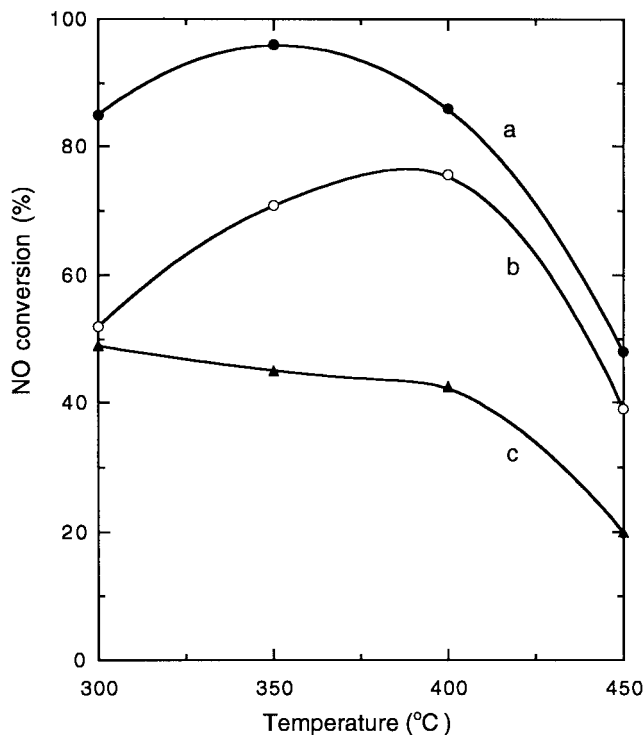


FIG. 2. SCR performance on (a) 10% $\text{Fe}_2\text{O}_3\text{-TiO}_2$ (SO_4^{2-}), (b) 5% $\text{Fe}_2\text{O}_3\text{-TiO}_2$ (SO_4^{2-}), and (c) 5% $\text{Fe}_2\text{O}_3\text{-TiO}_2$ catalysts under the conditions of 1000 ppm NO, 1000 ppm NH_3 , 2% O_2 , and $\text{GHSV} = 2.0 \times 10^5 \text{ h}^{-1}$.

SCR performance on $\text{Fe}_2\text{O}_3\text{-TiO}_2$ catalysts. Since $\text{Fe}_2\text{O}_3\text{-TiO}_2$ catalysts are known to be active for the SCR of NO with ammonia, we also investigated the SCR activities on the $\text{Fe}_2\text{O}_3\text{-TiO}_2$ catalysts prepared with the sol-gel method. $\text{Fe}_2\text{O}_3\text{-TiO}_2$ (5%), 5% $\text{Fe}_2\text{O}_3\text{-TiO}_2$ (SO_4^{2-}), and 10% $\text{Fe}_2\text{O}_3\text{-TiO}_2$ (SO_4^{2-}) were chosen for this study. NO conversions on these catalysts are shown in Fig. 2. Under the conditions of 1000 ppm NO, 1000 ppm NH_3 , 2% O_2 , and $\text{GHSV} = 2.0 \times 10^5 \text{ h}^{-1}$, NO conversions increased in the following order: 5% $\text{Fe}_2\text{O}_3\text{-TiO}_2 < 5\%$ $\text{Fe}_2\text{O}_3\text{-TiO}_2$ (SO_4^{2-}) $< 10\%$ $\text{Fe}_2\text{O}_3\text{-TiO}_2$ (SO_4^{2-}). This is consistent with N_2 selectivity for the SCO reaction over these catalysts (Tables 2 and 3). The maximum SCR activity was obtained at 350°C on 10% $\text{Fe}_2\text{O}_3\text{-TiO}_2$ (SO_4^{2-}).

TPD of ammonia. The TPD profiles of ammonia on Fe_2O_3 -containing catalysts are shown in Fig. 3. On 5% $\text{Fe}_2\text{O}_3\text{-SiO}_2$, only a small amount of ammonia was desorbed at 115°C. This may be related to its low surface area. For the other samples, ammonia desorption was observed over the wide temperature range of 50–450°C, indicating a broad distribution of sites for ammonia adsorption. The NH_3 desorbed at low temperatures may be assigned to physically adsorbed NH_3 and that desorbed at high temperature may be related to the chemisorbed NH_3 . A quantitative analysis using 1.07% NH_3/He as standard gas indicated that the amount of NH_3 desorption decreased in the relative order

of $\text{Fe}_2\text{O}_3\text{-Al}_2\text{O}_3$ (0.28 mmol/g) $> \text{Fe}_2\text{O}_3\text{-TiO}_2$ (0.19 mmol/g), $\text{Fe}_2\text{O}_3\text{-ZrO}_2$ (0.18 mmol/g) $> \text{Fe}_2\text{O}_3\text{-SiO}_2$ (0.05 mmol/g). This is in line with their surface area (Table 1). During the ammonia TPD experiments, only a trace amount of N_2 was produced above 350°C, but other oxidation products (such as N_2O or NO_x) were not detected.

The ammonia TPD profiles on 1–20% $\text{Fe}_2\text{O}_3\text{-TiO}_2$ (SO_4^{2-}) are shown in Fig. 4. Similar to $\text{Fe}_2\text{O}_3\text{-TiO}_2$ prepared with iron nitrate, these samples also showed a wide temperature range for ammonia desorption. However, a large amount of N_2 formation was observed at around 430°C. The amount of N_2 formation increased with the amounts of iron and sulfur (Fig. 5). But other oxidation products, e.g., N_2O or NO_x , were not detected. This indicates that lattice oxygen can oxidize ammonia adsorbed species to nitrogen at high temperatures. The amount of ammonia desorption (including oxidation product N_2) increased from 0.20 to 0.38 mmol/g with increasing Fe_2O_3 content from 1 to 20% on the catalysts (Figs. 4 and 5). Also, 5% $\text{Fe}_2\text{O}_3\text{-TiO}_2$ (SO_4^{2-}) (0.23 mmol/g) showed more ammonia desorption than 5% $\text{Fe}_2\text{O}_3\text{-TiO}_2$ (0.19 mmol/g).

TPSR between O_2 and ammonia adsorbed species. Figure 6 shows the TPSR results between ammonia adsorbed species and O_2 on 5% $\text{Fe}_2\text{O}_3\text{-TiO}_2$. NH_3 desorption was significant at low temperatures (i.e., below 300°C). At high temperatures, the reaction between O_2 and NH_3 adsorbed species occurred, producing N_2 and H_2O . The

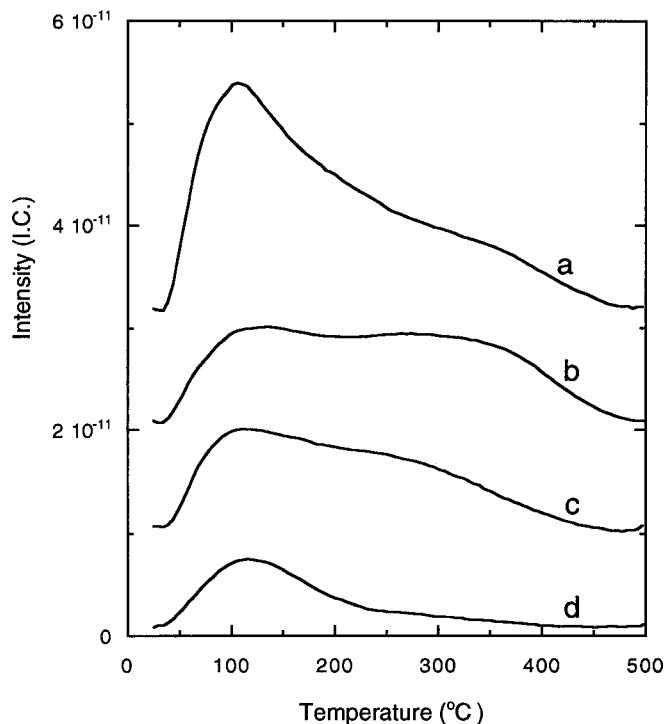


FIG. 3. TPD profiles of ammonia from (a) 5% $\text{Fe}_2\text{O}_3\text{-Al}_2\text{O}_3$, (b) 5% $\text{Fe}_2\text{O}_3\text{-TiO}_2$, (c) 5% $\text{Fe}_2\text{O}_3\text{-ZrO}_2$, and (d) 5% $\text{Fe}_2\text{O}_3\text{-SiO}_2$.

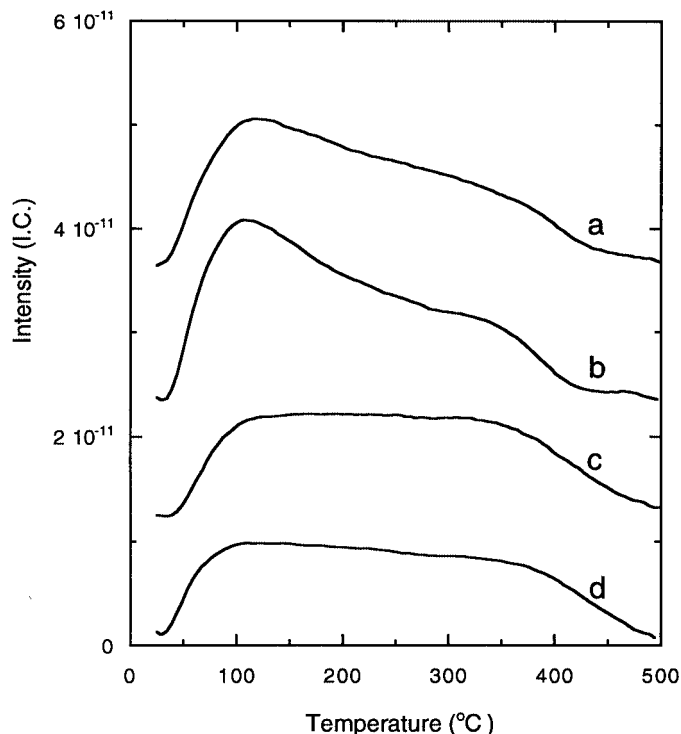


FIG. 4. TPD profiles of ammonia from (a) 20, (b) 10, (c) 5, and (d) 1% Fe₂O₃-TiO₂ (SO₄²⁻) catalysts.

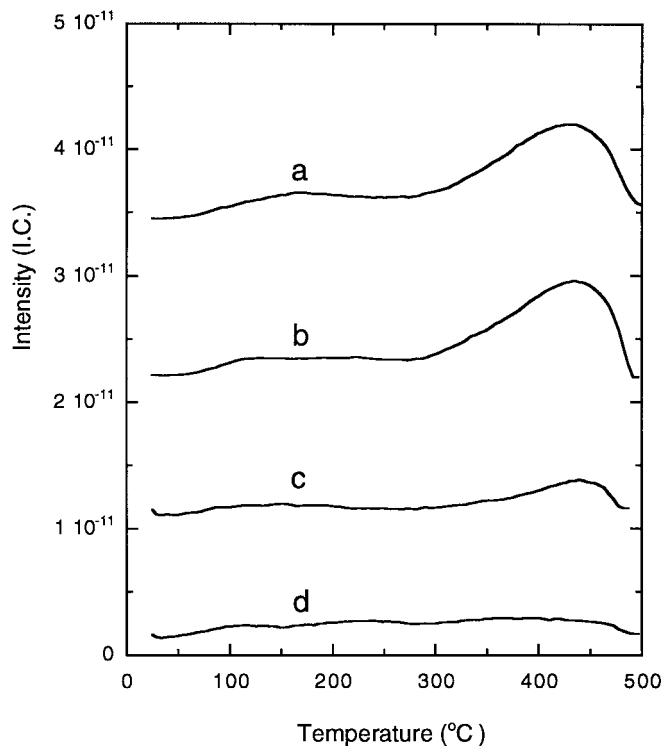


FIG. 5. N₂ formation during TPD of ammonia from (a) 20, (b) 10, (c) 5, and (d) 1% Fe₂O₃-TiO₂ (SO₄²⁻) catalysts.

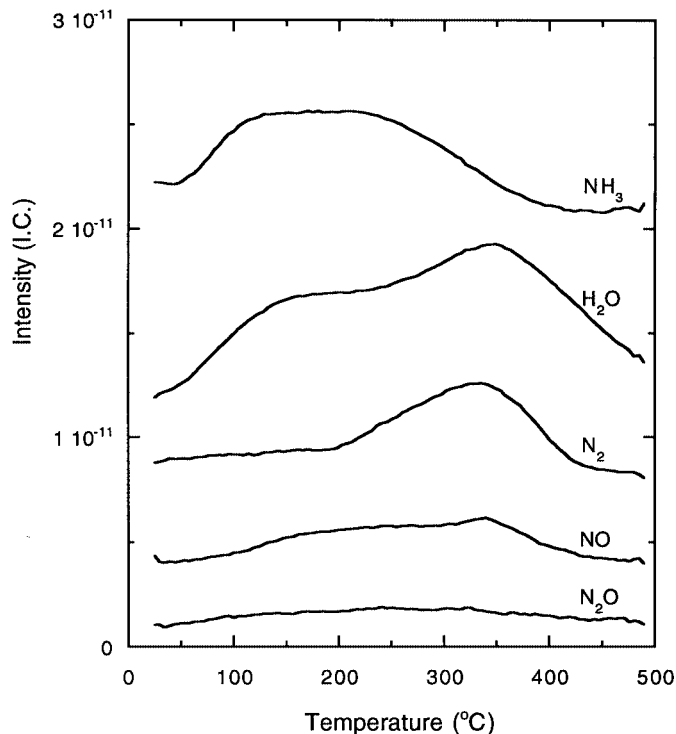


FIG. 6. TPSR profiles in 5% O₂ following exposure of 5% Fe₂O₃-TiO₂ to 1.07% NH₃/He for 60 min.

maximum N₂ production appeared at 330°C. Also, a small amount of NO was formed at high temperatures. N₂O was not detected in this experiment. The observation of H₂O at below 200°C is due to adsorbed H₂O (an impurity in 1.07% NH₃/He) because no other oxidation product of ammonia (e.g., N₂ or NO) was observed.

Similar results were obtained on 10% Fe₂O₃-TiO₂ (SO₄²⁻). NH₃ desorption dominated at low temperatures. At above 300°C, O₂ oxidized ammonia adsorbed species to nitrogen and water. The oxidation peak temperature appeared at 370°C. Almost no N₂O or NO was observed in the entire process.

DISCUSSION

The above results showed that Fe₂O₃-containing mixed oxides prepared from the sol-gel route were highly active for the SCO of ammonia to nitrogen. They could convert all of the ammonia to N₂ and NO at high temperatures, with N₂ as the major product. The N₂ selectivity and yield were found to increase in a trend of 5% Fe₂O₃-SiO₂ < 5% Fe₂O₃-ZrO₂ < 5% Fe₂O₃-TiO₂ < 5% Fe₂O₃-Al₂O₃ < 5% Fe₂O₃-TiO₂ (SO₄²⁻) < 10% Fe₂O₃-TiO₂ (SO₄²⁻), 20% Fe₂O₃-TiO₂ (SO₄²⁻) (Tables 2 and 3). The catalysts prepared with iron sulfate were more selective for N₂ than those prepared with nitrate. More than 92% of N₂ yields were obtained on the 10% Fe₂O₃-TiO₂ (SO₄²⁻) and 20% Fe₂O₃-TiO₂ (SO₄²⁻) at 400–450°C under the

condition of $\text{GHSV} = 2.0 \times 10^5 \text{ h}^{-1}$. They were more active than $\text{Ni}/\text{Al}_2\text{O}_3$ (3) but less active than Fe-exchanged zeolites (10, 11) for the conversion of NH_3 to N_2 . H_2O only decreased N_2 yield slightly due to a decrease in N_2 selectivity (Table 4). The ammonia TPD profiles showed that NH_3 could adsorb on a variety of acid sites of these catalysts and they desorbed over a wide temperature range (Figs. 3 and 4). The ammonia adsorbed species include physically adsorbed NH_3 (which was desorbed at low temperatures) and chemisorbed NH_3 . The coordinated NH_3 is probably the main form of chemisorbed ammonia because only Lewis acid sites were found on Fe_2O_3 , TiO_2 , and $\text{Fe}_2\text{O}_3/\text{TiO}_2$ (15). However, when sulfated, strong Brønsted acid sites were formed on TiO_2 (16) and Fe_2O_3 (14). Therefore, NH_4^+ ions are probably present on the $\text{Fe}_2\text{O}_3\text{-TiO}_2$ (SO_4^{2-}) catalysts. The foregoing IR spectra showed that sulfate species were present on the $\text{Fe}_2\text{O}_3\text{-TiO}_2$ (SO_4^{2-}) catalysts after calcination (Fig. 1). In the case of sulfate ions, $\text{S}=\text{O}$ has a covalent double bond and has a much stronger affinity to electrons compared with that of a simple metal sulfate; hence, the Lewis acid strength of metal ion becomes substantially stronger by the inductive effect of $\text{S}=\text{O}$ in the complex (14, 17). When a water molecule is bonded to the Lewis acid site, the Lewis acid site becomes a Brønsted acid site. Also, sulfate species provided new sites for ammonia adsorption, forming NH_4^+ ions. All of these will increase surface acidity and acid strength of the catalysts containing Fe_2O_3 and TiO_2 after sulfation. By comparing surface acidity (via ammonia TPD, Figs. 3 and 4) and SCO performance (Tables 2 and 3), we can see that the surface acidity has no bearing on the NH_3 conversion, while it is consistent with the N_2 selectivity and yield, i.e., the higher the surface acidity, the higher the N_2 yield.

It is significant that the Fe_2O_3 -containing catalysts also showed good activities for SCR of NO with ammonia. The SCR activities increased with the sequence of 5% $\text{Fe}_2\text{O}_3\text{-TiO}_2 < 5\% \text{ Fe}_2\text{O}_3\text{-TiO}_2$ (SO_4^{2-}) $< 10\% \text{ Fe}_2\text{O}_3\text{-TiO}_2$ (SO_4^{2-}) (Fig. 2), which is in good agreement with their surface acidity (Figs. 3 and 4) and N_2 selectivity for the SCO reaction (Tables 2 and 3). This observation suggests a correlation among them. It is noted that a high Fe content on the 10% $\text{Fe}_2\text{O}_3\text{-TiO}_2$ (SO_4^{2-}) also has beneficial effect on the SCR activity at low temperatures (14). The SCR of NO with NH_3 has been widely studied on many materials, such as mixed oxides and molecular sieves. Most researchers believe that strong surface acidity is beneficial to NH_3 adsorption and SCR activity, although which ammonia adsorbed species (NH_4^+ or coordinated NH_3) is involved in the reaction is still under debate (12, 15). The higher surface acidity results in a higher SCR activity on 5% $\text{Fe}_2\text{O}_3\text{-TiO}_2$ (SO_4^{2-}) than on 5% $\text{Fe}_2\text{O}_3\text{-TiO}_2$. Also, the 5% $\text{Fe}_2\text{O}_3\text{-TiO}_2$ showed a higher NO selectivity in the SCO reaction than did 5% $\text{Fe}_2\text{O}_3\text{-TiO}_2$ (SO_4^{2-}), especially at 350 and 400°C (Tables 2 and 3). Hence in the SCR re-

action, the NO generating from NH_3 oxidation by O_2 on the latter would be lower than that on the former. The decrease in NO formation on the sulfur-containing catalyst will also “increase” the apparent NO conversion. In the SCO reaction, when NO (the main by-product) is generated during the SCO reaction, it can be further reduced to N_2 by the unreacted ammonia adsorbed species through the SCR reaction. This finding supports the two-step SCO mechanism in which NO is an intermediate for N_2 formation (4, 11). NH_3 was first oxidized to NO by O_2 . This reaction occurs either on the catalyst surface or in the gaseous phase, or both. Our empty-tube results showed that NH_3 conversions were 23–55% at 350–450°C under the condition with 500 ml/min of total flow rate, with NO as the predominant product (10). Gaseous NH_3 mainly contributes to NO formation, which was proven on Fe-exchanged pillared clays in our previous work (9). Subsequently, the formed NO reacts with NH_3 adsorbed species to produce N_2 through the SCR reaction. Therefore, good SCR catalysts are expected to have high N_2 selectivities for the SCO reaction. An increase in surface acidity enhances ammonia adsorption and thus decreases the concentration of gaseous NH_3 . Since NO is mainly generated from gaseous NH_3 oxidation by O_2 (9, 10), less gaseous NH_3 will result in less NO formation. Simultaneously, more NH_3 (i.e., NH_3 adsorbed species) will be used to reduce NO. Of course this will improve SCR activity and N_2 selectivity for the SCO reaction. However, water also adsorbs on the catalyst competitively and enhances sulfur removal under the reaction conditions. This will increase the concentration of gaseous NH_3 and thus increase NH_3 oxidation to NO and decrease N_2 selectivity, as shown in Table 4.

In addition, the above TPD results also showed that lattice oxygen could oxidize the ammonia adsorbed species to N_2 on the $\text{Fe}_2\text{O}_3\text{-TiO}_2$ (SO_4^{2-}) catalysts (Fig. 5), indicating that lattice oxygen may be one of the active oxygen species for the SCO reaction at high temperatures. Over the catalysts prepared with iron nitrate, only a trace amount of N_2 was formed during TPD experiments. This is related to the fact that most of the ammonia desorbed from the surface at high temperatures, prior to oxidation, due to their weaker acidities. The reaction temperature (430°C) with lattice oxygen during TPD experiments (Fig. 5) was higher than those (330 and 370°C) in the presence of gaseous oxygen during TPSR experiments. This suggests that gaseous and/or adsorbed oxygen species may also participate in the SCO reaction at lower temperatures. The variable valence of iron cations on the Fe_2O_3 -containing catalysts might be beneficial to oxygen adsorption and activation. The oxygen adsorbed species, e.g., O_2^- , $\text{O}_2^{\delta-}$ ($1 < \delta < 2$), and O_2^{2-} , were observed on O_2 -adsorbed Fe_2O_3 by IR spectroscopy (18). The adsorption and activation of oxygen on the $\text{Fe}_2\text{O}_3\text{-TiO}_2$ SCO catalysts need to be verified by further spectroscopic characterization.

CONCLUSIONS

The Fe₂O₃-containing mixed oxides prepared from a sol-gel route were highly active for the SCO of ammonia to nitrogen. The catalysts prepared from iron sulfate were more selective for N₂ than those prepared from nitrate. The N₂ selectivity for the SCO reaction was in good agreement with their surface acidity as well as SCR activity. More than 92% of N₂ yields were obtained on the 10% Fe₂O₃-TiO₂ (SO₄²⁻) and 20% Fe₂O₃-TiO₂ (SO₄²⁻) at 400–450°C under the condition of GHSV = 2.0 × 10⁵ h⁻¹. The gaseous, adsorbed, and lattice oxygen all participated in the SCO reaction.

ACKNOWLEDGMENT

This work was supported by the Electric Power Research Institute and NSF Grant CTS-0095909.

REFERENCES

1. Il'chenko, N. I., *Russian Chem. Rev.* **45**, 1119 (1976).
2. Li, Y., and Armor, J. N., *Appl. Catal. B* **13**, 131 (1997).
3. Amblard, M., Burch, R., and Southward, B. W. L., *Appl. Catal. B* **22**, L59 (1999).
4. Amblard, M., Burch, R., and Southward, B. W. L., *Catal. Today* **59**, 365 (2000).
5. Sazonova, N. N., Simakov, A. V., Nikoro, T. A., Barannik, G. B., Lyakhova, V. F., Zheivot, V. I., Ismagilov, Z. R., and Veringa, H., *React. Kinet. Catal. Lett.* **57**, 71 (1996).
6. Gang, L., van Grondelle, J., Anderson, B. G., and van Santen, R. A., *J. Catal.* **186**, 100 (1999).
7. Curtin, T., O'Regan, F., Deconinck, C., Knuttle, N., and Hodnett, B. K., *Catal. Today* **55**, 189 (2000).
8. Wollner, A., and Lange, F., *Appl. Catal. A* **94**, 181 (1993).
9. Long, R. Q., Chang, M. T., and Yang, R. T., *Appl. Catal. B* **33**, 97 (2001).
10. Long, R. Q., and Yang, R. T., *Chem. Commun.* 1651 (2000).
11. Long, R. Q., and Yang, R. T., *J. Catal.* **201**, 145 (2001).
12. Bosch, H., and Janssen, F., *Catal. Today* **2**, 369 (1988).
13. Arata, K., in "Advance in Catalysis," Vol. 37, p. 165. Academic Press, San Diego, 1990.
14. Long, R. Q., and Yang, R. T., *J. Catal.* **186**, 254 (1999).
15. Busca, G., Lietti, L., Ramis, G., and Berti, F., *Appl. Catal. B* **18**, 1 (1998).
16. Chen, J. P., and Yang, R. T., *J. Catal.* **139**, 277 (1993).
17. Yamaguchi, T., *Appl. Catal.* **61**, 1 (1990).
18. Al-Mashta, F., Sheppard, N., Lorenzelli, V., and Busca, G., *J. Chem. Soc., Faraday Trans. I* **18**, 979 (1982).